

Research Article

Fixed-bearing Medial Unicompartmental Knee Arthroplasty Restores Neither the Medial Pivoting Behavior Nor the Ligament Forces of the Intact Knee in Passive Flexion[†]

Mohammad Kia¹, Lucian C. Warth², Joseph D. Lipman¹, Timothy M. Wright¹,

Geoffrey H. Westrich³, Michael B. Cross³, David J. Mayman³, Andrew D. Pearle⁴, Carl W. Imhauser¹

¹*Department of Biomechanics, Hospital for Special Surgery, 535 E. 70th St, New York, NY 10021*

²*Orthopaedic Surgery, Indiana University Health, 200 Hawkins Dr., Iowa City, IA 52242*

³*Adult Reconstruction and Joint Replacement Division, Hospital for Special Surgery, 535 E. 70th St, New York, NY 10021*

⁴*Sports Medicine, Hospital for Special Surgery, 535 E. 70th St, New York, NY 10021*

Corresponding Author:

Carl W. Imhauser, PhD
Biomechanics Department
Hospital for Special Surgery
535 E 70th St, New York, NY 10021

Tel: 212 606 1079

Fax: 212 606 1490

e-mail: ImhauserC@hss.edu

[†]This article has been accepted for publication and undergone full peer review but has not been through the copyediting, typesetting, pagination and proofreading process, which may lead to differences between this version and the Version of Record. Please cite this article as doi: [10.1002/jor.23838]

Additional Supporting Information may be found in the online version of this article.

Received 5 July 2016; Revised 20 June 2017; Accepted 26 August 2017

Journal of Orthopaedic Research

This article is protected by copyright. All rights reserved

DOI 10.1002/jor.23838

This article is protected by copyright. All rights reserved

Author Contribution Statement

All authors (Drs. Kia, Warth, Lipman, Wright, Westrich, Cross, Mayman, Pearle, and Imhauser) conceptualized and designed the study. Drs. Kia, Imhauser, and Warth carried out the study with computational modeling conducted by Dr. Kia. All authors contributed to data interpretation.

Drs. Warth, Imhauser, and Kia drafted the manuscript with all authors providing critical reviews and edits. All authors read and approved the final submitted manuscript.

Abstract:

Medial unicompartmental knee arthroplasty (UKA) is an accepted treatment for isolated medial osteoarthritis. However, using an improper thickness for the tibial component may contribute to early failure of the prosthesis or disease progression in the unreplaced lateral compartment. Little is known of the effect of insert thickness on both knee kinematics and ligament forces. Therefore, a computational model of the tibiofemoral joint was used to determine how non-conforming, fixed bearing medial UKA affects tibiofemoral kinematics and tension in the medial collateral ligament (MCL) and the anterior cruciate ligament (ACL) during passive knee flexion. Fixed bearing medial UKA could not maintain the medial pivoting that occurred in the intact knee from 0° to 30° of passive flexion. Abnormal anterior-posterior (AP) translations of the femoral condyles relative to the tibia delayed coupled internal tibial rotation, which occurred in the intact knee from 0° to 30° flexion, but occurred from 30° to 90° flexion following UKA. Increasing or decreasing tibial insert thickness following medial UKA also failed to restore the medial pivoting behavior of the intact knee despite modulating MCL and ACL forces. Reduced AP constraint in non-conforming medial UKA relative to the intact knee leads to abnormal condylar translations regardless of insert thickness even with intact cruciate and collateral ligaments. This finding suggests that the conformity of the medial compartment as driven by the medial meniscus and articular morphology plays an important role in controlling AP condylar translations in the intact tibiofemoral joint during passive flexion. This article is protected by copyright. All rights reserved

Keywords: medial pivoting, condylar translations, medial unicompartmental knee arthroplasty, overstuffed, ligament balancing, understuffed, insert thickness, ligament forces

Introduction

Medial unicompartmental knee arthroplasty (UKA) is an accepted treatment for patients with isolated medial osteoarthritis, in part because it has the potential to restore joint function more closely to normal than a total knee replacement¹⁻³. However, installing a medial UKA alters the shape, conformity, and stiffness of the medial compartment. Therefore, UKA perturbs the constraint provided by the medial compartment thereby altering kinematics compared to the intact tibiofemoral joint (i.e., a knee with unreplaced articular surfaces and all passive restraints including cruciate and collateral ligaments, and menisci). For example, we and others previously showed that installing a fixed-bearing, nonconforming UKA causes external rotation of the tibia relative to the femur and increased anterior-posterior (AP) translation of the medial femoral condyle compared to the intact knee joint^{3:4}. Thus, the screw home motion, a characteristic feature of intact knee function, was disturbed⁵.

Moreover, surgeons often adjust the thickness of the polyethylene tibial insert intraoperatively to restore the joint line and adjust ligament tension⁶ to ultimately avoid early failure of the prosthesis or progression of disease in the unreplaced lateral compartment⁷. However, the effect of adjusting tibial insert thickness on the biomechanical function of the knee, specifically the forces carried by the medial collateral ligament (MCL) and the anterior cruciate ligament (ACL), and the resulting kinematics through a range of flexion, are not well understood. A previous biomechanical study of UKA that integrated cadaveric testing and computational modeling reported the effect of adjusting tibial insert thickness on ligament strains and contact stress at full extension⁸, but the interaction between tibiofemoral kinematics and ligament forces through a range of flexion was not described. Previous studies have reported

This article is protected by copyright. All rights reserved

that increasing the thickness of the polyethylene (PE) tibial insert lengthens the distance between the attachments of the superficial MCL during simulated activities in a cadaver model⁹.

However, this measurement does not define the length at which the ligament begins to carry force; therefore, it is not a surrogate for ligament strain or force. Moreover, no previous studies identified the interaction between tibial insert thickness and ACL loading; which also plays a critical role in knee kinematics¹⁰. Altogether, *in vitro* measurement of ligament forces are challenging in the setting of numerous permutations in implant alignment and the propensity for tissue degradation with time, while ligament forces are extremely difficult to measure *in vivo*¹¹.

To provide a more comprehensive description of the effects of tibial component thickness in UKA on knee kinematics and on ligament forces, we used a previously developed computational model of the tibiofemoral joint together with subject-specific experimental data. We addressed the following research questions: 1) Can the computational model accurately predict AP translations of the medial and lateral femoral condyles relative to the tibia? 2) How does tibial insert thickness affect AP translations of the medial and lateral femoral condyles, axial rotation of the tibia, as well as MCL and ACL forces compared to that of the intact knee?

Methods

A previously developed multibody computational model of an intact tibiofemoral joint¹² was adapted for the current study and used in two main phases to address our research questions. First, the AP translations of the medial and lateral femoral condyles relative to the tibia were compared to a corresponding cadaveric experiment; and second, a fixed bearing UKA was virtually installed and the effect of implant thickness on tibiofemoral kinematics and ligament

This article is protected by copyright. All rights reserved

forces was assessed. For the first phase, the computational model of the intact knee consisted of subject-specific geometries of the tibia, femur, articular cartilage, and menisci from a 20 year-old male cadaveric knee obtained from computed tomography (CT) scanning (Fig. 1a).

Fig. 1 Here

A total of 42 ligament fibers described the cruciate and collateral ligaments, capsular structures, and horn and coronary attachments of the menisci¹³⁻¹⁶. The ligament fibers were modeled with non-linear, tension-only springs connecting the femur to the tibia and the menisci to the tibia. Mean structural properties were employed to describe the force-elongation response of the fibers including toe and subsequent linear regions¹⁷⁻²⁰. The slack length of each fiber was determined using a previously-described algorithm¹². The MCL was represented with anterior, central, and posterior fibers: each divided into distal and proximal pairs¹². Each pair of the MCL fibers was modeled to wrap around the proximal tibia (Fig. 1a)¹². The lateral and medial meniscal geometries were discretized radially, and a linear stiffness matrix connected neighboring elements to represent a deformable geometry as described by Guess et al.²¹. Tibiomeniscal coronary ligaments were modeled with seven tension-only linear fibers on the medial side and one fiber on the lateral side¹². The coronary ligaments connect the tibial plateau to the outer aspects of the lateral and medial menisci²². Each meniscus has an anterior and posterior horn attachment that connects the ends of the menisci to the tibial plateau²². Rigid body contact was defined as a non-linear function of penetration depth and penetration velocity between opposing cartilage surfaces and between meniscal and cartilage surfaces^{12; 21; 23}.

Passive knee flexion (i.e., flexing the knee without applying muscle forces) was simulated because it is an important intraoperative assessment used by surgeons to appraise the

This article is protected by copyright. All rights reserved

interaction of articular surfaces and the soft tissue structures that span the tibiofemoral joint. To simulate passive flexion, the femur was flexed about its transepicondylar axis, while the tibia was allowed rotation and translation in all directions except in flexion-extension. The femur was flexed from full extension to 90° of flexion at a rate of 0.9°/s to reflect the slow rate of loading used in a corresponding cadaveric experiment¹². A compressive force of 10 N was maintained across the joint throughout flexion, again to simulate the physical experiment. The compressive force was applied along the long axis of the tibia, which was defined by digitizing previously-described anatomical landmarks¹². These landmarks consisted of the sulcus of the fibular head, the MCL about 2 cm below the medial joint line, and the tibial shaft about 15 cm distal to the joint line. The long axis was directed distally and was defined using the bisection of the two proximal landmarks and the distal landmark described above. The equations of motion were solved using the multibody dynamics software ADAMS (MSC Software, Santa Ana, CA) employing a GSTIFF integration scheme²⁴.

Previously, predicted mechanics of the intact tibiofemoral joint agreed with cadaveric measurements obtained in a robotic simulator including anterior translation and internal rotation (≤ 0.4 mm and 1.6° root mean square (RMS) error, respectively) and collateral and cruciate ligament forces (≤ 5.7 N RMS error) from full extension to 130° flexion¹². Extending this previous work, we compared the predicted AP translations of the medial and lateral femoral condyles with respect to the tibia with corresponding data from a cadaveric experiment, since these outcome measures are a common means of describing tibiofemoral kinematics in knee arthroplasty applications²⁵. The medial and lateral condyles were respectively represented by tracking the most prominent peaks on the medial and lateral sides of the femur (i.e., the femoral epicondyles) as has been previously utilized (Fig. 1B)²⁵. The AP translations of these points

This article is protected by copyright. All rights reserved

were determined relative to an AP-oriented vector. The direction of this vector was defined as the common perpendicular of the line connecting the medial and lateral femoral epicondyles (i.e., the transepicondylar axis or TEA) and the long axis of the tibia; a decreasing value with respect to the intact knee indicated posterior translation of the femoral condyles relative to the tibia. Internal/external rotation of the tibia was described relative to the femur by adapting the convention of Grood and Suntay^{26; 27}. Resultant forces carried by the MCL and ACL were predicted by the model during passive flexion.

To answer the first research question concerning the ability of the computational knee model to accurately predict AP translations of the medial and lateral femoral condyles relative to the tibia, a cadaveric experiment was conducted using a previously described six degrees of freedom robot^{12; 27} on the same intact knee specimen that was modeled. All loads, boundary conditions, and coordinate systems were consistent across the model and experiment¹². The differences between predicted and experimentally measured AP translations of the medial and lateral femoral condyles relative to the tibia were calculated in 1° increments throughout the entire flexion path. The root mean square (RMS) difference between experimental measurements and model predictions were reported from 0° to 30°, 30° to 60°, and 60° to 90° flexion to assess the ability of the model to capture AP translations in extension, midflexion, and deeper flexion, respectively.

To answer our second research question concerning the effects of tibial insert thickness on tibiofemoral biomechanics, a fixed bearing medial UKA was virtually implanted into the computational model. Then, the sensitivity of the outcomes to the thickness of the tibial insert was evaluated. The 3D shapes of the femoral and tibial components of a Stryker Triathlon™ fixed-bearing UKA (Mahwah, NJ) were captured using a laser scanner (Konica Minolta, Inc,

This article is protected by copyright. All rights reserved

Tokyo, Japan; accuracy: $\pm 40 \mu\text{m}$, precision: $4 \mu\text{m}$). 3D modeling software packages (Geomagic Studio, Geomagic, Inc., Research Triangle Park, NC and SolidWorks, Dassault Systèmes, Waltham, MA) were used to convert the point cloud data from the scanner to a 3D surface in Parasolid format (Fig. 2A).

Fig. 2 Here

Next, a fellowship-trained arthroplasty surgeon aligned the femoral and tibial components to the CT-derived articular surfaces at full extension by manipulating the components in 3D using image processing software (Mimics, Materialise, Inc., Belgium). This approach yielded a femoral component in 3° extension relative to the mechanical axis of the femur. The tibial component was perpendicular to the mechanical axis in the coronal plane and had 6° of posterior slope in the sagittal plane (Fig. 2B). After placing the UKA in the multibody dynamics model, rigid body contact between the tibiofemoral articular surfaces was defined. The stiffness of the contact interface was modeled using a two-parameter power function based on a uniaxial compression test (Supplementary Material, Appendix 1, Fig. S-1 and S-2).

To create a *balanced* knee, the tibial polyethylene insert was translated proximally to match the MCL tension to that of the intact model in full extension. This approximated the surgical goal of restoring MCL tension with UKA implantation²⁸. The component was then translated in the proximal-distal direction from this *balanced* position by $\pm 2 \text{ mm}$ to simulate surgically *over-* and *understuffing* the joint by changing the tibial insert thicknesses (Fig. 3).

Fig. 3 Here

This article is protected by copyright. All rights reserved

The knee models with the UKA implanted underwent passive flexion as described above, and the AP translations of the lateral and medial femoral condyles with respect to the tibia, tibial axial rotation with respect to the femur, and forces carried by the ACL and MCL were calculated (Fig. 3). The changes in tibiofemoral kinematics imparted by the *balanced*, *overstuffed*, and *understuffed* UKA were reported in two flexion ranges relative to the intact knee: 0-30° flexion to assess medial pivoting in extension, and 30-90° to assess the remainder of the passive flexion range.

Results

The *in silico* model of the intact knee predicted AP translations of the medial and lateral femoral condyles that agreed with those measured *in vitro*. Predicted AP translations of the medial femoral condyle differed from the cadaveric experiment by 0.8, 2.0, and 1.7 mm RMS from 0° to 30°, 30° to 60°, and 60° to 90° flexion, respectively (Fig. 4).

Fig. 4 Here

Model predictions of AP translations of the lateral femoral condyle differed from the cadaveric experiment by 1.4, 2.4, and 2.4 mm RMS from 0° to 30°, 30° to 60°, and 60° to 90° flexion, respectively.

The *balanced*, *overstuffed*, and *understuffed* UKA failed to reproduce the AP translations of the medial and lateral femoral condyles of the intact knee (Fig. 5).

Fig. 5 Here

With the UKA in a *balanced* position, the posterior translation of the medial and lateral femoral condyles was 8.6 mm more and 6.1 mm less, respectively, than the intact knee from 0° to 30° flexion. *Overstuffing* the UKA led to minimal AP translation of the medial femoral condyle of 0.1 mm from 0° to 30° flexion. With the *understuffed* UKA, the medial femoral condyle translated 14.4 mm more posteriorly compared to the intact knee from 0° to 30° of flexion, while the lateral condyle translated 7.8 mm less posteriorly than in the intact knee from 0° to 30° of flexion. With regards to axial rotation from 0° to 30° of flexion, internal tibial rotation decreased compared to the intact knee in the *balanced*, *overstuffed*, and *understuffed* UKA, by 11.0°, 7.0° and 17.0°, respectively (Fig. 6).

Fig. 6 Here

Compared to the intact knee, the medial and lateral femoral condyles of the *balanced* UKA translated a respective 4.4 mm less and 7.4 mm more posteriorly from 30° to 90° flexion (Fig.5). By *overstuffing* the UKA, the medial femoral condyle translated 2.9 mm less posteriorly compared to the intact knee from 30° to 90° flexion, while the lateral femoral condyle translated 6.7 mm more posteriorly. By *understuffing* the UKA the medial femoral condyle translated 5.2 mm less posteriorly compared to the intact knee from 30° to 90° flexion, and the lateral femoral condyle translated 7.6 mm more posteriorly. Internal tibial rotation in the *balanced*, *overstuffed*, and *understuffed* UKA from 30° to 90° flexion was 9.0°, 7.0° and 10.0° greater, respectively, than the intact knee (Fig. 6).

This article is protected by copyright. All rights reserved

In the intact knee, the predicted MCL forces remained low from 0° to 90° passive flexion, ranging from 1 to 8 N (Fig. 7).

Fig. 7 Here

For the *balanced* UKA, the predicted MCL force was similar to that of the intact knee at full extension (6 N) and at 90° flexion (8 N). Between full extension and 90° flexion, the predicted MCL force was higher in the *balanced* UKA than in the intact knee by up to 10 N. *Overstuffing* the medial compartment increased MCL force by at least 38 N in full extension relative to the intact knee and the MCL remained taut from 0° to 90° of flexion. The MCL force in the *understuffed* knee dropped to 0 N at full extension and remained unloaded until 20° of flexion. From 20° to 90° flexion, the MCL force in the *understuffed* UKA was lower than the intact knee, notably by 6 N at 90° flexion.

In the intact knee, ACL force was maximum in full extension, reaching 25 N, and decreased to 0 N as the knee flexed to 90° (Fig. 8).

Fig. 8 Here

The predicted ACL force with the *balanced* UKA was 10 N higher than the intact knee in full extension and up to 8 N higher across the flexion path. *Overstuffing* the medial compartment

This article is protected by copyright. All rights reserved

increased ACL force through the entire range of flexion compared to the intact knee by up to 45 N at full extension. *Understuffing* the medial compartment decreased ACL force in full extension by 7 N relative to the intact knee and paralleled that of the intact knee through the remainder of the flexion arc.

Discussion

A multibody model of the intact knee corroborated specimen-specific experimental measurements of AP translations of the femoral condyles during passive flexion and was subsequently used to assess knee function following UKA. The main findings of this study were that fixed bearing medial UKA could not maintain the medial pivoting that occurred in the intact knee from 0° to 30° of passive flexion (Fig. 5). These abnormal condylar translations delayed coupled internal rotation, which occurred in the intact knee from 0° to 30° flexion, but occurred from 30° to 75° flexion following UKA (Fig. 6). Importantly, the model provided predictions of MCL and ACL forces; although *overstuffing* the medial compartment partially restored medial pivoting of the intact knee, it increased MCL and ACL tension (Figs. 7, 8). In contrast, *understuffing* the medial compartment reduced MCL and ACL tension, but led to abnormal lateral pivoting in extension.

The increased posterior translation of the medial femoral condyle that we observed from 0° to 30° flexion after installing the medial UKA is most likely due to the flat shape of the tibial insert (Fig. 5). Without the medial meniscus to add concavity and AP restraint to the medial compartment, no mechanism is available following UKA to help maintain the AP translations of the medial condyle in extension^{29, 30}. Our results also suggest that even though UKA preserves

important ligamentous stabilizers such as the ACL, knee kinematics are still highly sensitive to the conformity of the replaced medial articular surfaces.

Modulating the forces carried by the ACL and MCL by *over-* or *understuffing* the medial compartment was inadequate in maintaining the AP translations of femoral condyles observed in the intact knee from 0° to 30° flexion. Specifically, even *overstuffing* the medial compartment, which increased MCL tension by at least 38 N and ACL tension by up to 45 N, could not control abnormal translations of the medial femoral condyle. Our results suggest that AP condylar translations in nonconforming medial UKA are difficult to control by changing implant thickness alone even with all major ligaments intact. These findings align with clinical reports of the difficulty in obtaining predictable knee kinematics when attempting to preserve the cruciate ligaments in knee replacement^{31; 32}.

Installing the medial UKA and perturbing insert thickness resulted in abnormal posterior translations of the lateral femoral condyle. Specifically, after UKA, the lateral femoral condyle translated less posteriorly from 0° to 30° flexion and more posteriorly from 30° to 90° flexion than the intact knee (Fig. 5). This caused coupled internal tibial rotation to occur from 30° to 90° instead of from 0° to 30° following UKA (Fig. 6). These findings were similar to Heyse et al. where posterior translations of the lateral compartment following medial UKA implantation decreased in the *understuffed* UKA^{3; 9}.

The findings of abnormal condylar translations following UKA may indicate subtle joint instability and aberrant articular contact mechanics. Increased AP translations of the medial femoral condyle could lead to failure of the prosthesis through wear and aseptic loosening, while abnormal translations of the lateral femoral condyle could accelerate progression of osteoarthritic

This article is protected by copyright. All rights reserved

changes in the unreplaced compartment³³⁻³⁵. We speculate that our findings of subtle kinematic deficits in extension may also help explain previous reports that 10% of individuals felt unsafe or anxious when participating in sporting activities following UKA³⁶.

Previous studies reported coupled internal tibial rotation with flexion in the intact knee ranging from 14 to 36° from full extension to approximately 100° knee flexion⁵. This finding agrees with our results: internal rotation of 14° in the intact knee from 0° to 90° flexion. Our model predicted 11.2° of tibial external rotation from 0° to 30° of flexion after UKA implantation in a balanced position, which also agrees with a previous cadaveric study⁴.

Overstuffing the UKA was previously shown to reduce valgus laxity and increase valgus stiffness³⁷. This effect of UKA is likely due to the increased MCL and ACL tension reported in the present study⁹. Thus, *overstuffing* should likely be avoided. *Understuffing* the medial UKA by 2 mm should probably be avoided as well; it exacerbated the abnormal posterior translation of the medial and lateral femoral condyles observed with the balanced UKA during passive flexion, likely due to increased slack in the MCL and ACL. Although placing the UKA in the *balanced* position maintained the forces in the MCL in the intact knee in full extension and at 90° flexion, the forces were increased at all other angles throughout the flexion path. Altogether, a *balanced* fixed-bearing UKA did not capture the low ligament forces observed in the MCL and ACL during passive flexion^{12; 38}.

In contrast to our findings, Patil et al.³⁹ suggested that a nonconforming medial UKA design (PreservationTM; DePuy, Johnson and Johnson, Warsaw, IN) preserves both axial rotation of the tibia and femoral rollback during a closed kinetic chain knee extension. However, the additional constraint of their test set-up, which did not allow translation of the distal tibia, likely

This article is protected by copyright. All rights reserved

reduced the ability to detect changes in articular geometry compared to our less constrained model. Similar to our findings, Heyse et al. identified increased posterior translation of the medial femoral condyle after installing the UKA in comparison to the intact knee using a less constrained loading rig³.

Our study has limitations. A model of a single knee does not represent the extent of bony and articular morphologies and ligament shapes and mechanical properties present across a population. However, the model underwent rigorous evaluation against subject-specific experimental measurements both in this study and previously¹². From 0° to 30° flexion, the 0.8 mm RMS difference between predicted and measured AP translations of the medial femoral condyle was eighteen times less than the differences imparted by installing the UKA in any of the three positions. Similarly, the 1.4 mm RMS difference between predicted and experimentally measured AP translations of the lateral condyle was five times less than the predicted differences caused by installing the UKA and changing insert thickness. The model also corroborated experimental findings of AP translations of the medial and lateral femoral condyles of the intact knee¹² and abnormal external rotation with passive flexion in a group of ten similarly-tested knee specimens undergoing UKA⁴. Thus, we believe that the conclusions derived using the model are strong. A second limitation was that the simulations included low compressive forces, reflecting those applied in the exam and operating rooms, not those encountered during daily activities. Nevertheless, our simple model of passive flexion was able to identify the influence of altered medial compartment conformity and tibial insert thickness in UKA on tibiofemoral kinematics and ligament forces.

This study has further limitations. A rigid body contact formulation was utilized, which neglects the deformation of the articular surfaces; however, the model does account for the stiffness of both the contacting cartilage surfaces²¹ and the contacting metal and polyethylene components (Supplementary Material, Appendix 1, Fig. S-1 and S-2). Furthermore, our simulations utilized frictionless articular surfaces. We assessed the impact of including both static and dynamic friction between the contacting metal and polyethylene surfaces in the model utilizing values for the dynamic (0.035) and static friction (0.04) coefficients measured as a function of slip velocity⁴⁰. We found that for the overstuffed UKA, which generated the greatest medial contact force and is therefore the worst case scenario, that the ACL and MCL forces changed by <1 N at any single flexion angle after including friction. Similarly, AP translations of the medial and lateral condyles differed by <0.7 mm and <0.1 mm, respectively, at any angle of knee flexion (Supplementary Material, Appendix 2, Fig. S-3). In contrast, the changes in AP translations, from 0° to 90°, between the *balanced*, *over-*, and *understuffed* UKA was a minimum of 7.2 mm, in the medial compartment which is ten times larger than the difference caused by including friction. Nevertheless, subsequent analyses can easily include friction. The current work focused on quantifying the effect of *overstuffing* and *understuffing* of the medial compartment in a single UKA design. Therefore, our findings are not generalizable to other designs such as those using a mobile bearing; future studies could easily integrate different articular shapes.

In summary, installing a fixed bearing medial UKA in a computational model of the tibiofemoral joint corroborated previous findings of altered AP translations of the medial and lateral femoral condyles. Modulating tibial insert thickness via *overstuffing* or *understuffing* the joint line following medial UKA also failed to restore the medial pivoting behavior of the intact

This article is protected by copyright. All rights reserved

knee. Unique to this study using a computational model, we found that *overstuffing* comes at the cost of increased MCL and ACL tension, which would elevate contact force on the medial compartment. On the other hand, *understuffing* the joint line reduced MCL and ACL tension, but caused lateral pivoting in extension. This computational knee model can be used to understand the interaction between common variables that are surgically manipulated such as implant placement and the resulting function of the knee including kinematics and ligament forces.

Acknowledgment

The financial support for this study was provided by the Dr. and Mrs. Leonard Marmor Fund and the Clark and Kirby Foundations. Although unrelated to this study, the authors have the following disclosures. Dr. Timothy Wright receives royalties from Mathys ABG, Lima Inc., Wolters Kluwer, and Exactech Inc., and serves as a consultant for Zimmer and a scientific advisory board for Orthobond Corporation. Dr. Geoffrey Westrich serves as a consultant for Don Joy Orthopedics, Exactech Inc. and Stryker Corp. Dr. Michael Cross serves as a consultant for Smith & Nephew, Acclivity, Exactech Inc., Intellijoint Surgical Inc., and LinkBio Corp. Dr. David Mayman serves as a consultant for Mako, Orthalign, and Smith & Nephew. Dr. Andrew Pearle serves as a consultant for Biomet Inc., Stryker, and Mako Surgical Corp. and serves on the scientific advisory board for Blue Belt Technologies, Inc.

References

1. Zuiderbaan HA, van der List JP, Khamaisy S, et al. 2015. Unicompartmental knee arthroplasty versus total knee arthroplasty: Which type of artificial joint do patients forget? *Knee Surg Sports Traumatol Arthrosc*.
2. McAllister CM. 2008. The role of unicompartmental knee arthroplasty versus total knee arthroplasty in providing maximal performance and satisfaction. *J Knee Surg* 21:286-292.
3. Heyse TJ, El-Zayat BF, De Corte R, et al. 2014. UKA closely preserves natural knee kinematics in vitro. *Knee Surg Sports Traumatol Arthrosc* 22:1902-1910.
4. Cassidy KA, Tucker SM, Rajak Y, et al. 2015. Kinematics of passive flexion following balanced and overstuffed fixed bearing unicondylar knee arthroplasty. *Knee* 22:542-546.
5. Wilson DR, Feikes JD, Zavatsky AB, et al. 2000. The components of passive knee movement are coupled to flexion angle. *J Biomech* 33:465-473.
6. Edwards SA, Pandit HG, Ramos JL, et al. 2002. Analysis of polyethylene thickness of tibial components in total knee replacement. *J Bone Joint Surg Am* 84-A:369-371.
7. Price AJ, Svard U. 2011. A second decade lifetable survival analysis of the Oxford unicompartmental knee arthroplasty. *Clin Orthop Relat Res* 469:174-179.
8. Innocenti B, Bilgen OF, Labey L, et al. 2014. Load sharing and ligament strains in balanced, overstuffed and understuffed UKA. A validated finite element analysis. *J Arthroplasty* 29:1491-1498.
9. Heyse TJ, El-Zayat BF, De Corte R, et al. 2015. Balancing UKA: overstuffing leads to high medial collateral ligament strains. *Knee Surg Sports Traumatol Arthrosc*.
10. Matsumoto H, Suda Y, Otani T, et al. 2001. Roles of the anterior cruciate ligament and the medial collateral ligament in preventing valgus instability. *J Orthop Sci* 6:28-32.
11. Holden JP, Grood ES, Korvick DL, et al. 1994. In vivo forces in the anterior cruciate ligament: direct measurements during walking and trotting in a quadruped. *J Biomech* 27:517-526.
12. Kia M, Schafer K, Lipman J, et al. 2016. A Multibody Knee Model Corroborates Subject-Specific Experimental Measurements of Low Ligament Forces and Kinematic Coupling During Passive Flexion. *J Biomech Eng* 138.
13. Ziegler CG, Pietrini SD, Westerhaus BD, et al. 2011. Arthroscopically pertinent landmarks for tunnel positioning in single-bundle and double-bundle anterior cruciate ligament reconstructions. *Am J Sports Med* 39:743-752.
14. LaPrade RF, Engebretsen AH, Ly TV, et al. 2007. The anatomy of the medial part of the knee. *J Bone Joint Surg Am* 89:2000-2010.
15. LaPrade RF, Morgan PM, Wentorf FA, et al. 2007. The anatomy of the posterior aspect of the knee. An anatomic study. *J Bone Joint Surg Am* 89:758-764.
16. Lopes OV, Jr., Ferretti M, Shen W, et al. 2008. Topography of the femoral attachment of the posterior cruciate ligament. *J Bone Joint Surg Am* 90:249-255.
17. Butler DL, Guan Y, Kay MD, et al. 1992. Location-dependent variations in the material properties of the anterior cruciate ligament. *J Biomech* 25:511-518.
18. Robinson JR, Bull AM, Amis AA. 2005. Structural properties of the medial collateral ligament complex of the human knee. *J Biomech* 38:1067-1074.

19. Harner CD, Xerogeanes JW, Livesay GA, et al. 1995. The human posterior cruciate ligament complex: an interdisciplinary study. Ligament morphology and biomechanical evaluation. *Am J Sports Med* 23:736-745.
20. Wilson WT, Deakin AH, Payne AP, et al. 2012. Comparative analysis of the structural properties of the collateral ligaments of the human knee. *J Orthop Sports Phys Ther* 42:345-351.
21. Guess TM, Thiagarajan G, Kia M, et al. 2010. A subject specific multibody model of the knee with menisci. *Med Eng Phys* 32:505-515.
22. Brindle T, Nyland J, Johnson DL. 2001. The meniscus: review of basic principles with application to surgery and rehabilitation. *J Athl Train* 36:160-169.
23. Imhauser CW, Siegler S, Udupa JK, et al. 2008. Subject-specific models of the hindfoot reveal a relationship between morphology and passive mechanical properties. *J Biomech* 41:1341-1349.
24. Gear CW. 1971. Simultaneous Numerical Solution of Differential Algebraic Equations. *IEEE Trans Circuit Theory* 18:89 - 95
25. Feng Y, Tsai TY, Li JS, et al. 2016. In-vivo analysis of flexion axes of the knee: Femoral condylar motion during dynamic knee flexion. *Clin Biomech (Bristol, Avon)* 32:102-107.
26. Grood ES, Suntay WJ. 1983. A joint coordinate system for the clinical description of three-dimensional motions: application to the knee. *J Biomech Eng* 105:136-144.
27. Imhauser C, Mauro C, Choi D, et al. 2013. Abnormal tibiofemoral contact stress and its association with altered kinematics after center-center anterior cruciate ligament reconstruction: an in vitro study. *Am J Sports Med* 41:815-825.
28. Khamaisy S, Zuiderbaan HA, van der List JP, et al. 2016. Medial unicompartmental knee arthroplasty improves congruence and restores joint space width of the lateral compartment. *Knee* 23:501-505.
29. Levy IM, Torzilli PA, Warren RF. 1982. The effect of medial meniscectomy on anterior-posterior motion of the knee. *J Bone Joint Surg Am* 64:883-888.
30. Allen CR, Wong EK, Livesay GA, et al. 2000. Importance of the medial meniscus in the anterior cruciate ligament-deficient knee. *J Orthop Res* 18:109-115.
31. Banks S, Bellemans J, Nozaki H, et al. 2003. Knee motions during maximum flexion in fixed and mobile-bearing arthroplasties. *Clin Orthop Relat Res*:131-138.
32. Fantozzi S, Catani F, Ensini A, et al. 2006. Femoral rollback of cruciate-retaining and posterior-stabilized total knee replacements: in vivo fluoroscopic analysis during activities of daily living. *J Orthop Res* 24:2222-2229.
33. Berger RA, Meneghini RM, Jacobs JJ, et al. 2005. Results of unicompartmental knee arthroplasty at a minimum of ten years of follow-up. *J Bone Joint Surg Am* 87:999-1006.
34. Weale AE, Murray DW, Baines J, et al. 2000. Radiological changes five years after unicompartmental knee replacement. *J Bone Joint Surg Br* 82:996-1000.
35. Tochigi Y, Vaseenon T, Heiner AD, et al. 2011. Instability dependency of osteoarthritis development in a rabbit model of graded anterior cruciate ligament transection. *J Bone Joint Surg Am* 93:640-647.
36. Naal FD, Fischer M, Preuss A, et al. 2007. Return to sports and recreational activity after unicompartmental knee arthroplasty. *Am J Sports Med* 35:1688-1695.
37. Heyse TJ, Tucker SM, Rajak Y, et al. 2015. Frontal plane stability following UKA in a biomechanical study. *Arch Orthop Trauma Surg* 135:857-865.

38. Markolf KL, Gorek JF, Kabo JM, et al. 1990. Direct measurement of resultant forces in the anterior cruciate ligament. An in vitro study performed with a new experimental technique. *J Bone Joint Surg Am* 72:557-567.
39. Patil S, Colwell CW, Jr., Ezzet KA, et al. 2005. Can normal knee kinematics be restored with unicompartmental knee replacement? *J Bone Joint Surg Am* 87:332-338.
40. Schwenke T, Borgstede LL, Schneider E, et al. 2005. The influence of slip velocity on wear of total knee arthroplasty. *Wear* 259:926-932.

Figure Legends

Figure 1: A) Overview of the multibody model of the intact tibiofemoral joint including bony geometries, articular cartilage, discretized menisci, and ligament fibers; B) tibiofemoral kinematics were described by measuring the anterior-posterior translations of the medial and lateral femoral epicondyles relative to the tibia. The femoral epicondyles are marked with black and red circles at 0 and 90° flexion, respectively

Figure 2: A) The 3D geometries of the femoral and tibial components of a Stryker Triathlon™ fixed-bearing unicompartmental knee arthroplasty (UKA) captured using a laser scanner; and (B) virtually aligned UKA within the computational model according to surgeon recommendations (ligament fibers are not shown).

Figure 3: The computational model was passively flexed from 0° to 90° flexion with all soft tissues intact (Intact) and after replacing the medial compartment with unicompartmental knee arthroplasty (UKA), which was placed in *balanced*, *overstuffed* (2 mm thicker tibial insert), and *understuffed* (2 mm thinner tibial insert) positions. Outcomes compared across each condition were the AP translations of the medial and lateral femoral condyles relative to the tibia, axial rotation of the tibia relative to the femur, and forces carried by the MCL and ACL. Magnitude of ligament forces is indicated by the length of the red arrows.

Figure 4: Anterior-posterior (AP) translation of the medial and lateral femoral condyles relative to the tibia during passive flexion of the intact knee model (solid line, Model) and the corresponding cadaver experiment (dashed line, Experiment) on the same knee that was

modeled. A positive number indicates anterior translation of the femur relative to the tibia. (Ant = anterior, mm = millimeters)

Figure 5: Predicted anterior-posterior (AP) translations of the medial and lateral femoral condyles relative to the tibia at 0, 30, 60, and 90° of passive flexion in the intact (A, gold line), *balanced* (B, black line), 2 mm *overstuffed* (C, red line), and 2 mm *understuffed* (D, blue line) knee. Decreasing color intensity indicates increasing flexion for each condition. A positive number indicates anterior translation of the femur relative to the tibia. (mm = millimeters)

Figure 6: Predicted internal/external (axial) tibial rotation during passive flexion in the intact (gold solid line), *balanced* (black dashed line), 2 mm *overstuffed* (red solid line), and 2 mm *understuffed* (blue solid line) knee. A positive number indicates internal tibial rotation.

Figure 7: Predicted force carried by the medial collateral ligament (MCL) during passive flexion in the intact (gold solid line), *balanced* (black dashed line), 2 mm *overstuffed* (red solid line), and 2 mm *understuffed* (blue solid line) knee. N = Newtons.

Figure 8: Predicted force carried by the anterior cruciate ligament (ACL) during passive flexion in the intact (gold solid line), *balanced* (black dashed line), 2 mm *overstuffed* (red solid line), and 2 mm *understuffed* (blue solid line). N = Newtons.

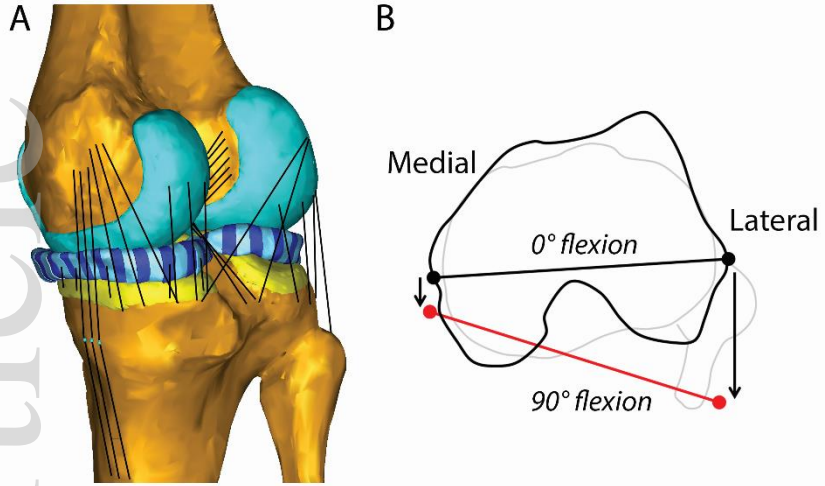


Figure 1

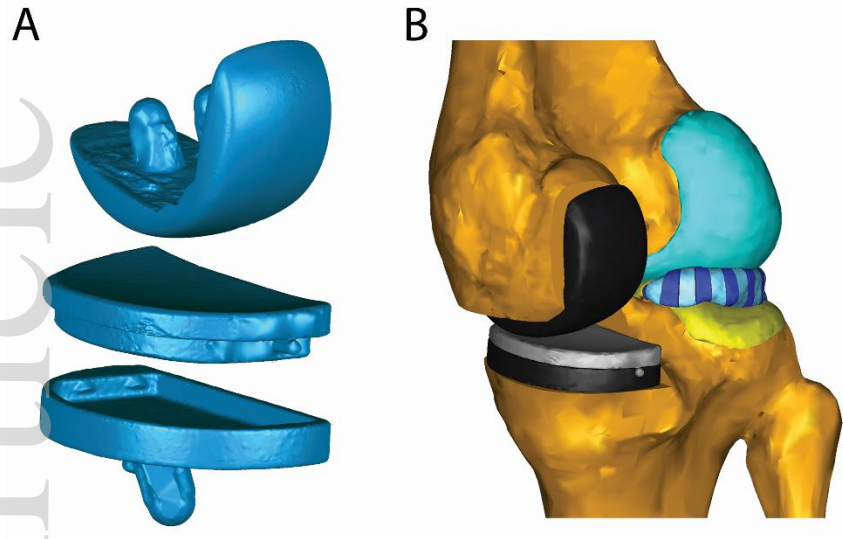


Figure 2

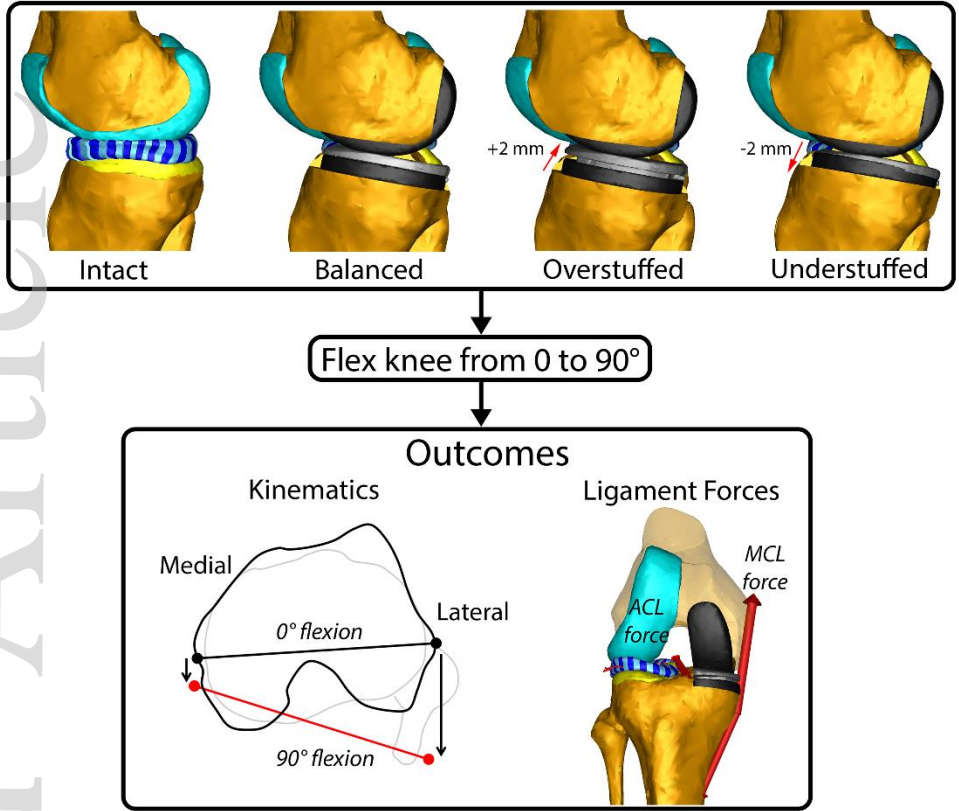


Figure 3

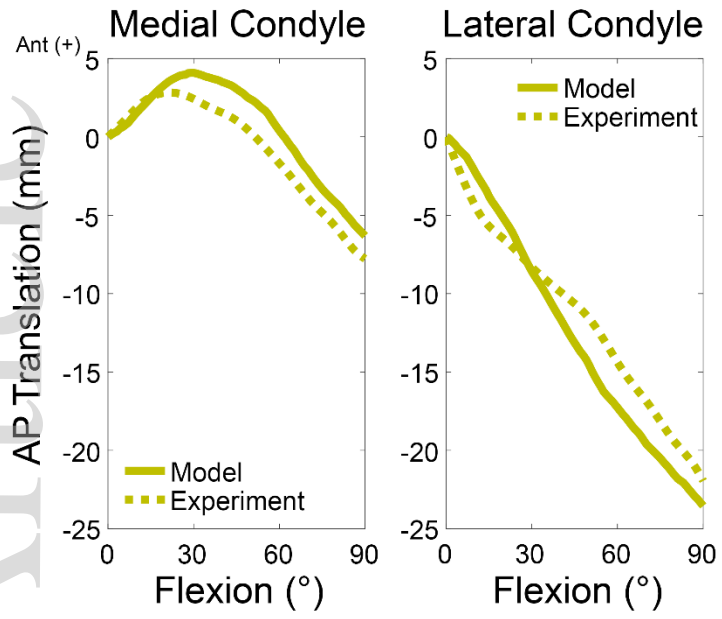


Figure 4

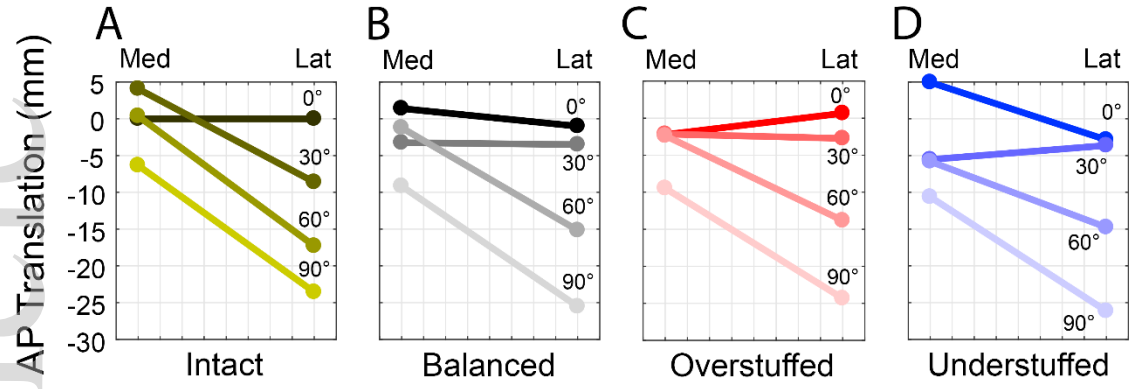


Figure 5

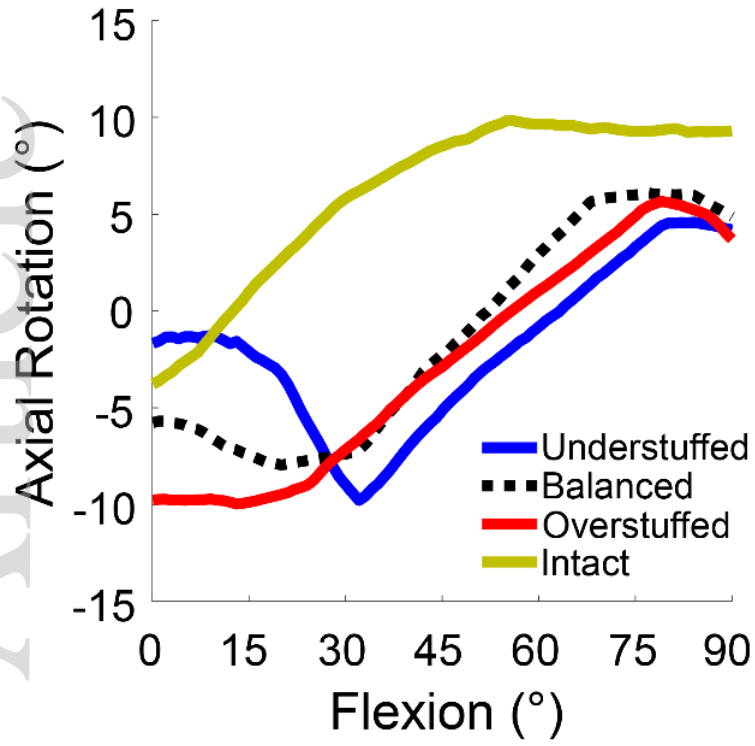


Figure 6

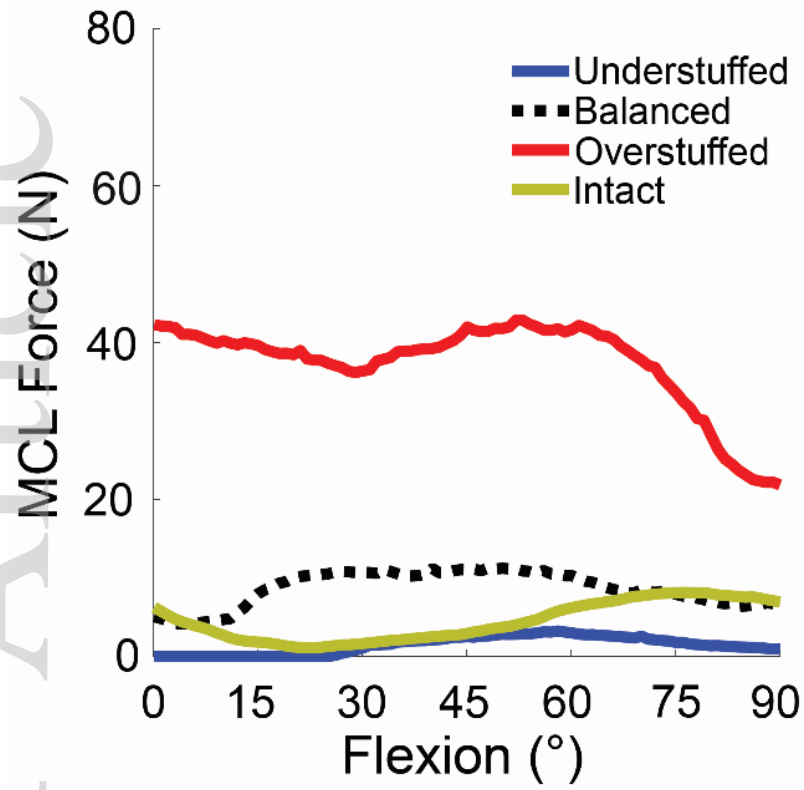


Figure 7

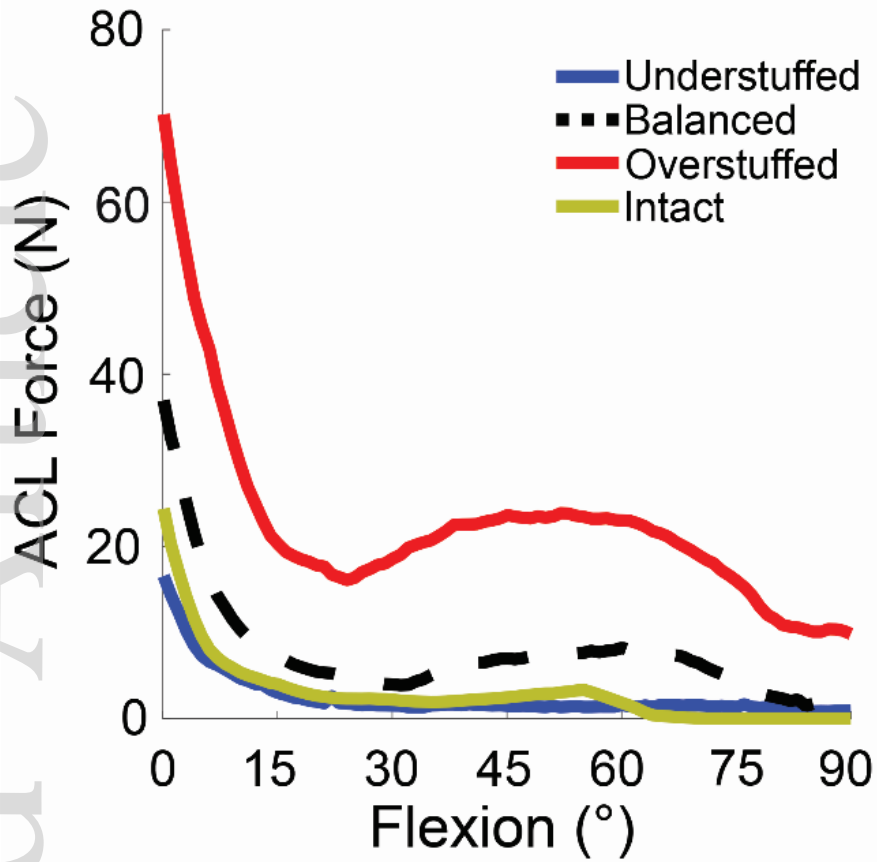


Figure 8